


RESEARCH

Open Access



Coupled Effect of Temperature and Strain Rate on Mechanical Properties of Steel Fiber-Reinforced Concrete

Ruiyuan Huang^{1*} , Shichao Li², Long Meng³, Dong Jiang⁴ and Ping Li⁵

Abstract

The dynamic mechanical properties of steel fiber-reinforced concrete (SFRC) under high temperature and high strain rate were studied using a split Hopkinson pressure bar (SHPB) of 74 mm in diameter. As it is difficult to achieve constant strain rate loading in SHPB experiments with high temperature and high strain rate, this paper first presents a method for determining the strain rate under non-constant strain rate loading conditions. This method is proposed to deal with experimental data under non-constant strain rate loading conditions. Then, the influences of temperature on the ultimate compressive strength, peak strain, and failure modes of SFRC under different strain rates were analyzed and the results show that SFRC has a strain rate hardening effect. This paper also points out that there is a strain rate threshold for SFRC. If the strain rate is less than the strain rate threshold, there is a temperature softening effect. Conversely, if the strain rate is greater than the strain rate threshold, there is a temperature hardening effect. Finally, the relationship between the ultimate compressive strength and fiber volume fraction, strain rate, and temperature is presented and the prediction results are consistent with the experimental data.

Keywords: steel fiber-reinforced concrete (SFRC), high temperature, high strain rate, split Hopkinson pressure bar (SHPB), ultimate compressive strength

1 Introduction

Steel fiber can increase the energy adsorption, crack resistance and impact strength of concrete significantly (Song and Hwang 2004; Yang et al. 2017; Holschemacher et al. 2010; Li et al. 2017a, b; Wang et al. 2008; El-Dieb 2009). It has been widely used in military and civilian applications such as pavements, tunnels, bridges and fortifications. These engineering structures may be exposed to fire and explosions in accidents and terrorist attacks (Chen et al. 2015; Liu and Xu 2013). Under these conditions, the circumstances surrounding the Steel fiber-reinforced concrete (SFRC) are very complex given the combined effect of the temperature field and dynamic

load. Therefore, it is of importance to conduct a study on the coupled effect of temperature and strain rate on the mechanical properties of SFRC.

Currently, the research is mainly focused on the mechanical properties of concrete after exposing it to high temperatures. Tai et al. (2011) investigated the stress–strain relationship in reactive powder concrete (RPC) under quasi-static loading after exposure to an elevated temperature, and the experimental results indicate that the residual compressive strength of RPC after heating it at 200–300 °C increases more than that at room temperature, but it significantly decreases when the temperature exceeds 300 °C. Dügenci et al. (2015) pointed out that the compressive strength, modulus of elasticity and toughness values of fiber-concrete substantially decreased by the effect of high temperature. Poon et al. (2004) showed that the compressive strength and stiffness of concrete will decrease when exposed to

*Correspondence: ryhuang@njust.edu.cn

¹ Assistant Professor in Nanjing University of Science and Technology, Jiangsu 210094, China

Full list of author information is available at the end of the article
Journal information: ISSN 1976-0485 / eISSN 2234-1315

elevated temperatures. Lau et al. (2006) reported that the steel fiber can improve both the fire resistance and crack resistance. Kim et al. (2015) studied the factors influencing the mechanical tensile properties of SFRC exposed to high temperatures and the results show that the residual compressive strength, tensile strength and rupture energy of the specimens decreased with increased heating. Xu et al. (2001) investigated the residual properties of pulverized fly ash (PFA) concrete after being subjected to high temperatures.

The high temperature and high strain rate effects on concrete have also been studied. Wang and Hao (2017) pointed out that the influence of temperature on peak stress and peak strain of rock is not evident below 500 °C, but the influence becomes remarkable at 700 °C and 900 °C. Su et al. (2014) showed that the dynamic compressive strength and specific energy absorption of concrete increase with the strain rate at different temperatures. Chen et al. (2015) showed that the appearances at failure of normal concrete subjected to both high temperature and high strain rate loading were significantly different from those of concrete at ambient temperature. Li et al. (2017a, b) found that the increase in strength of recycled aggregate concrete just slightly improves the impact properties of a recycled aggregate concrete-filled steel tube after exposure to elevated temperatures higher than 500 °C. At present, there is no consistent conclusion about the effect of temperature on the compressive properties of concrete. Siddique and Kaur (2012) showed that the compressive strength, splitting tensile strength and elasticity modulus of concrete have a temperature softening effect, and Çavdar (2012) pointed out that the compressive strengths of mortars reduce under high temperature. However, Pan et al. (2014) found that the strength of a geopolymer increased significantly in the range of 200–300 °C.

It is well-known that the mechanical properties of concrete have strong dependence on both the temperature and strain rate. In this study, to investigate the effect of

temperature, strain rate, and fiber volume fraction on the compressive properties of concrete, split Hopkinson pressure bar (SHPB) tests are performed on SFRC specimens by varying the values of treatment temperature and strain rate. As it is difficult to achieve constant strain rate loading in SHPB tests on SFRC specimens under high temperature and high strain rate, a method for determining the strain rate under non-constant strain rate loading conditions is first proposed to deal with the experimental data under such conditions. Then, the influence of temperature on ultimate compressive strength, peak strain and failure modes of SFRC under different strain rates are investigated based on the test results. Finally, the relationship between ultimate compressive strength and fiber volume fraction, strain rate, and temperature is also presented, which contributes to the design of SFRC engineering structures exposed to high temperature and high strain rate.

2 Experimental Investigation

2.1 Raw Materials and Specimen Preparation

In this investigation, to eliminate the effect of coarse aggregate particle size on the scale effect of the test piece, the maximum size of coarse aggregate was 8 mm. The river sand with the fineness modulus is of 2.30. The length and diameter of the steel fiber were 13 mm and 0.2 mm. Owing to the limitation of the mixing process, the steel fiber content of the currently commonly used SFRC is generally within 2%. However, to further study the effect of higher fiber content on the mechanical properties of SFRC, a higher fiber content is also designed. In this work, four different fiber volumes were added, that is, 0%, 0.75%, 1.5% and 4.5% by volume of concrete. Some raw materials are shown in Fig. 1 and the mix proportions are presented in Table 1. The specimens for the SHPB test have a diameter of 70 mm and a length of 35 mm to meet the assumption of stress uniformity (Dai et al. 2010). The parallelism between the top and bottom surface of the specimen is within 0.01 mm.

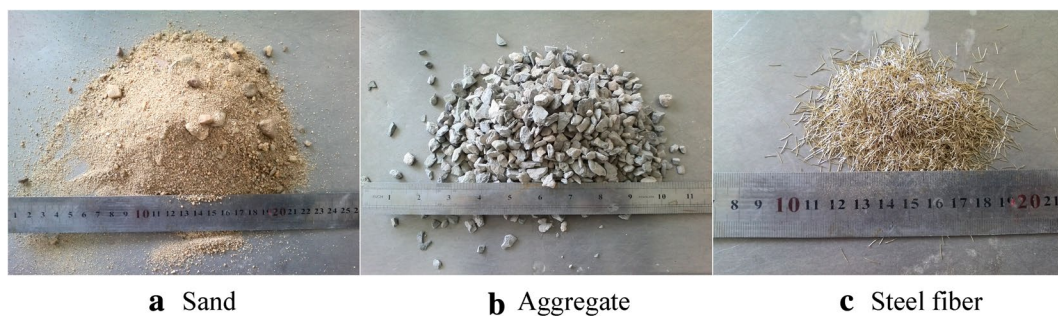


Fig. 1 Raw materials.

Table 1 Mix proportions design of SFRC.

Fiber volume fraction (%)	Cement (kg/m ³)	Sand (kg/m ³)	Steel fiber (kg/m ³)	Fly ash (kg/m ³)	Water (kg/m ³)	Aggregate (kg/m ³)
0	391	698	0	59	158	1090
0.75	450	676	58.5	68	182	1056
1.5	505	645	117	76	204	1004
4.5	693	470	351	105	280	726

2.2 Testing Methods and Testing Principle

The SHPB, as shown in Fig. 2, was adopted in this study. For the SHPB system used in this study, the lengths of the striker, incident, and transmission bars are 50, 5461, and 3485 mm, respectively. According to the wave propagation theory and two basic assumptions (Wu et al. 2010), the average stress, strain and strain rate of the SFRC specimen can be obtained by the following two-wave method (Xiao et al. 2015):

$$\sigma(t) = \frac{EA}{A_s} \varepsilon_t(t) \tag{1}$$

$$\varepsilon(t) = -\frac{2C_0}{l_0} \int_0^t \varepsilon_r(t) dt \tag{2}$$

$$\dot{\varepsilon}(t) = -\frac{2C_0}{l_0} \varepsilon_r(t) \tag{3}$$

where E and A are the elastic modulus and cross-sectional area of the SHPB bars, C_0 denotes the elastic wave velocity in bars, and A_s and l_0 represent the cross-sectional area and length of the SFRC specimen, respectively.

2.3 High Temperature Device

In this study, three groups of SFRC specimens were prepared including one obtained at room temperature and the other two treated at 200 °C and 400 °C, respectively. The SFRC specimens were heated to the specified temperature in a high-temperature furnace and kept for 30 min. In the course of the experiment, the other instruments were first commissioned; then, a specific fixture was used to quickly place the heated SFRC specimens in the designated position, and the impact test was performed immediately. As a type of thermal inert material, concrete has a very low heat transfer coefficient. The experimental results (Wang et al. 2014) show that the temperature of the concrete specimen with an initial temperature of 460 °C is only reduced by 20 °C after being placed at room temperature environment for 33 s. The entire process of the experiment takes 7 to 10 s with multi-person collaboration, and the temperature of the SFRC specimen is reduced by approximately 5 °C. Therefore, during the heating process, the specified temperatures were set to 205 °C and 405 °C, respectively.

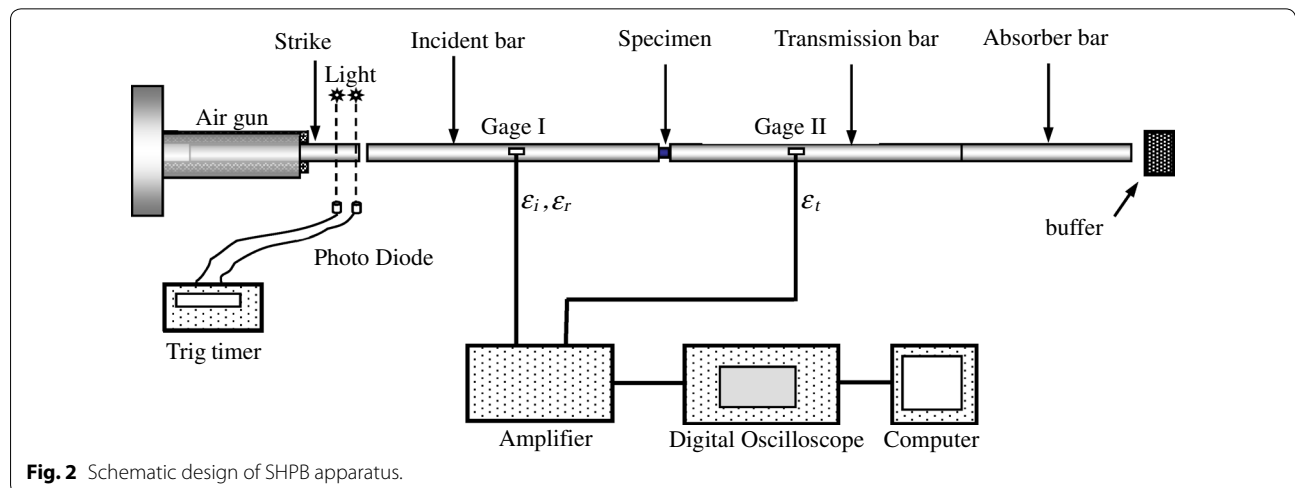


Fig. 2 Schematic design of SHPB apparatus.

3 Experimental Results and Discussion

3.1 Method for Determining Strain Rate of SFRC Specimen Under Non-constant Strain Rate Loading Conditions in SHPB Experiment

As a brittle material, the strain at failure of concrete is very small, usually only a few thousandths. The loading time of the dynamic mechanical properties experiments is very short, which poses a challenge to the application of the SHPB technology to concrete (Zhu et al. 2009). Frew et al. (2002) studied the SHPB experiment of brittle materials and used a shaper to solve the problem of stress uniformity. They also pointed out that the constant strain rate loading is difficult to achieve in the SHPB experiment of brittle materials. In this study, brass was used as a shaper to solve the problem of stress uniformity of the SFRC specimens in SHPB experiments. Constant strain rate loading of an SFRC specimen under lower strain rates can be achieved by adjusting the size of the brass, but it is difficult to achieve constant strain rate loading of the SFRC specimen under high temperatures and high strain rates. As a strain rate-sensitive material (Lv et al. 2018), the strain rate effect of concrete has an important influence on its constitutive model. Therefore, it is important to determine the strain rate corresponding to the experimental data of SFRC specimens under non-constant strain rate loading conditions in the SHPB experiment.

In the SHPB experiment, there are three main methods for determining the strain rate corresponding to the experimental data under non-constant strain rate loading conditions: (1) the average strain rate corresponding to the entire loading process (Tao et al. 2005); (2) the average strain rate corresponding to the specimen loading process up to the stress peak process (Li et al. 2008); (3) the average strain rate corresponding to the specimen loading process from 80% of the stress peak to the stress peak (Wang et al. 2012). These three methods for determining the strain rate have strong subjectivity, which brings certain errors to the study of the strain rate effect of materials.

Figure 3 shows the typical voltage signals obtained from the experiment. The corresponding stress–strain curve and strain rate history curve are shown in Fig. 4. It can be observed from Fig. 4 that the time required for the specimen to reach the constant strain rate loading section is 76 μs , and the corresponding stress at this moment is 50% of the peak stress. Ravichandran and Subhash (1994) concluded that the specimen reached a stress uniform state after the stress wave propagated three times back and forth in the specimen. Through calculation, the time that the stress wave propagates in the specimen for three times is $\Delta t = 57 \mu\text{s}$. The SHPB experimental data of SFRC achieves constant strain rate

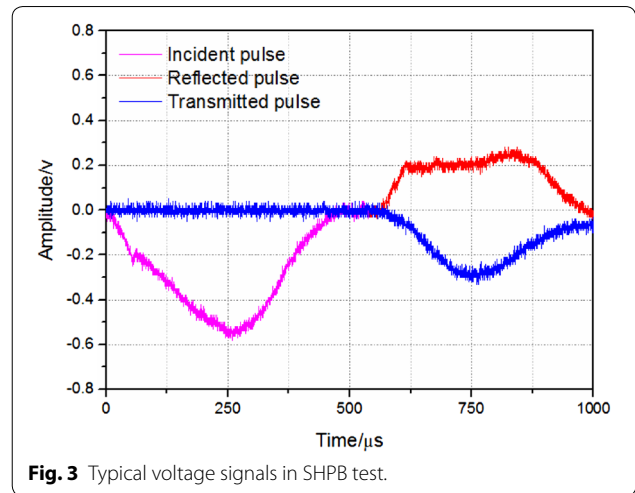


Fig. 3 Typical voltage signals in SHPB test.

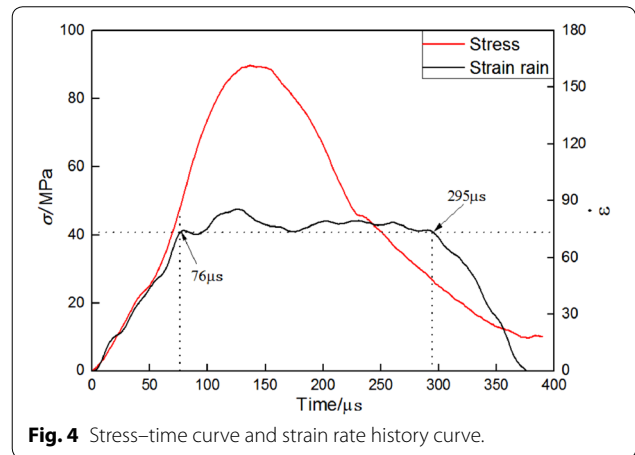
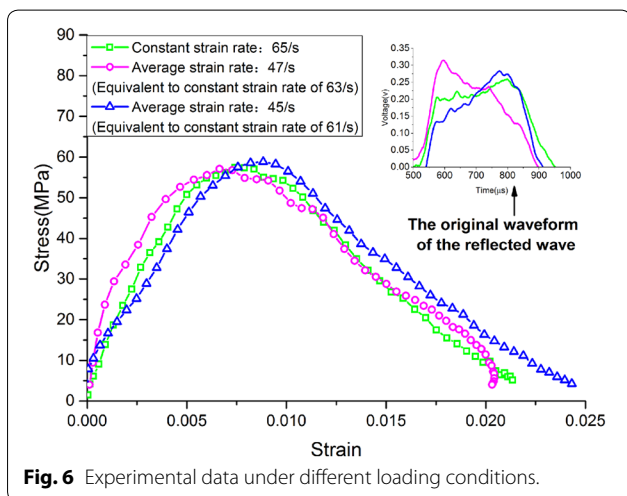
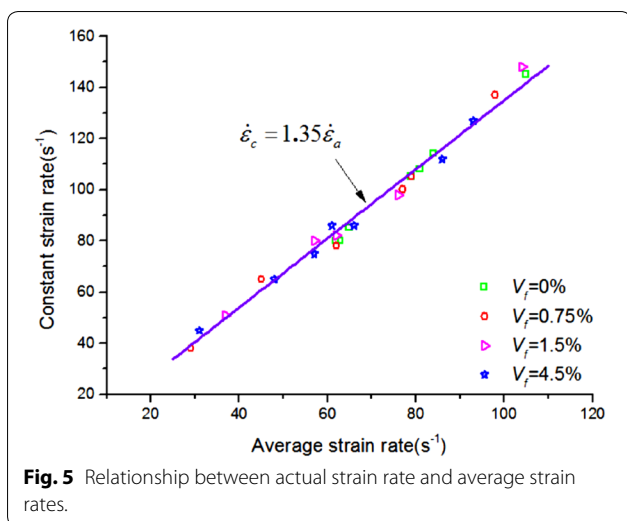


Fig. 4 Stress–time curve and strain rate history curve.

loading and satisfies the assumption of stress uniformity during loading.

In this study, more than 20 sets of experimental data under constant strain rate loading were obtained using brass as a shaper. A very interesting conclusion can be drawn by processing the SHPB experimental data under constant strain rate loading, as shown in Fig. 5, where the X-axis represents the average strain rate $\dot{\epsilon}_a$ corresponding to the experimental data under the entire loading process and the Y-axis represents the actual strain rate $\dot{\epsilon}_c$ corresponding to the experimental data. It can be observed from the figure that the actual strain rate can be expressed as the relationship of the average strain rate: $\dot{\epsilon}_c = 1.35\dot{\epsilon}_a$. Figure 6 shows the experimental data under three different loading conditions. It can be observed from the figure that when the experimental data have the same strain rate determined by $1.35\dot{\epsilon}_a$, the corresponding stress–strain curves are similar.



3.2 Data Analysis and Discussion

The stress–strain curves of SFRC with different fiber volume fractions (0%, 0.75%, 1.5%, and 4.5%) at different temperatures (20 °C, 200 °C, and 400 °C) obtained from the SHPB tests are plotted in Figs. 7, 8 and 9. These curves were calculated from the strain signals recorded in the bars using Eqs. (1)–(3).

The dynamic strength is defined as the ultimate compressive strength herein. It can be observed from the figures that both the ultimate compressive strength and the peak strain increase as the strain rate increases, and there is a significant strain rate effect at different temperatures.

At similar strain rates, the actual failure modes of SFRC with different steel fiber volume fractions at 20 °C

are presented in Fig. 10. The results show that the addition of steel fiber can improve the damage resistance of concrete. It can be concluded that the addition of steel fibers effectively improves the toughness of concrete.

The peak strain–strain rate curves of SFRC with different fiber volume fractions at different temperatures are shown in Fig. 11. The results show that the peak strain decreases as the strain rate increases at 20 °C, while the peak strain increases as the strain rate increases at 200 °C and 400 °C. The peak strain has the temperature effect, and the results show that the peak strain increases as the temperature increases.

The ultimate compressive strength (σ_c) is the maximum stress that a material can withstand under external forces and plays an extremely important role in determining the constitutive model of a brittle material such as SFRC. Figure 12 shows the ultimate compressive strength–strain rate curves of SFRC at different temperatures. The results show that the compressive strength of concrete increases with the increase in strain rate and there is a linear relationship between them (Dilger et al. 1984; Song and Lu 2012).

The strain rate effect of SFRC at a high temperature is more sensitive than that at room temperature. Experimental results show that there is a strain rate threshold for SFRC. The strain rate thresholds for SFRC with fiber volume fractions of 0%, 0.75%, 1.5%, and 4.5% are 76/s, 81/s, 61/s, and 70/s, respectively. When the strain rate is less than the strain rate threshold, the ultimate compressive strength decreases with the increase in temperature, indicating that it has a temperature softening effect. When the strain rate is greater than the strain rate threshold, the ultimate compressive strength increases with the increase in temperature, indicating that it has a temperature hardening effect. The moisture of the SFRC specimen escapes in the form of free water as the temperature increases, thereby increasing the porosity of the specimen. The difference in porosity will lead to changes in the mechanical properties of concrete at high temperatures. Therefore, the ultimate compressive strength of SFRC is a combination of temperature and strain rate.

The ultimate compressive strength of SFRC exhibits softening at low strain rates owing to the temperature softening effect. As the strain rate hardening effect at high temperatures is more pronounced, the ultimate compressive strength of SFRC exhibits hardening as the strain rate increases. The failure modes of SFRC with fiber volume fraction of 1.5% at different temperatures are shown in Fig. 13. The experimental results also show that the SFRC has better resistance to damage at high temperatures when the strain rate exceeds the strain rate threshold.

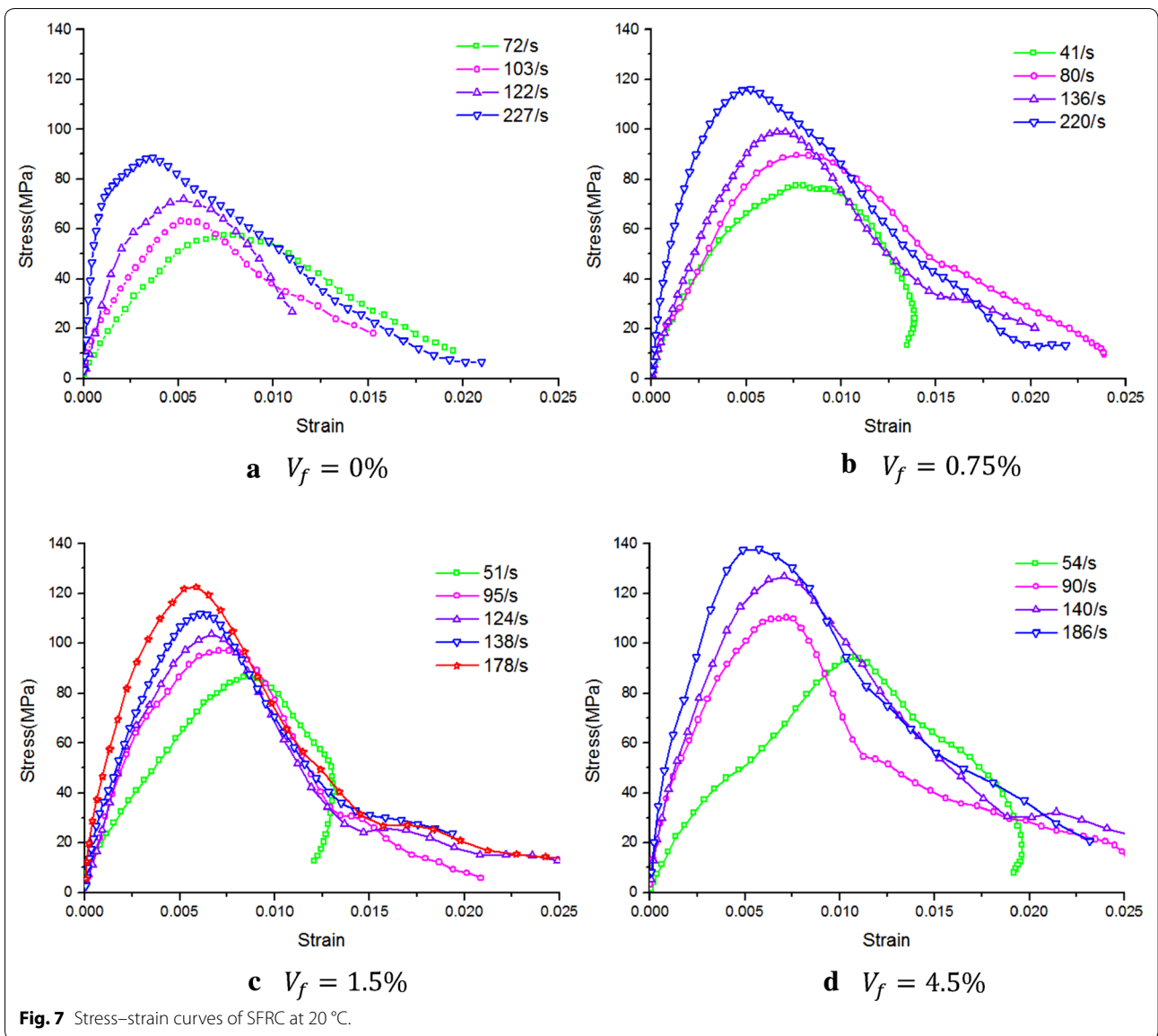


Fig. 7 Stress–strain curves of SFRC at 20 °C.

4 Relationship Between Ultimate Compressive Strength and Fiber Volume Fraction, Strain Rate, and Temperature

4.1 Expression of Ultimate Compressive Strength

The ultimate compressive strength (σ_c) is an important index to reflect the dynamic mechanical properties of SFRC. Figure 14 shows the ultimate compressive strength–strain rate curves of SFRC at different temperatures. The experimental results show that the ultimate compressive strength increases with the increase in strain rate and the addition of steel fiber, and it also has the temperature effect.

Experimental results show that the ultimate compressive strength and strain rate have a linear relationship. The addition of steel fiber increases the ultimate compressive strength, but with the increase in fiber volume fraction, its growth gradually slows down, showing a power function relationship. Therefore, there is the following relationship between ultimate compressive strength and fiber volume fraction, strain rate, and temperature:

$$\sigma_c = f(\dot{\epsilon})g(V_f) = \left(A + B \frac{\dot{\epsilon}}{\dot{\epsilon}_0} \right) \left[1 + C \left(\frac{V_f}{V_0} \right)^D \right] \quad (4)$$

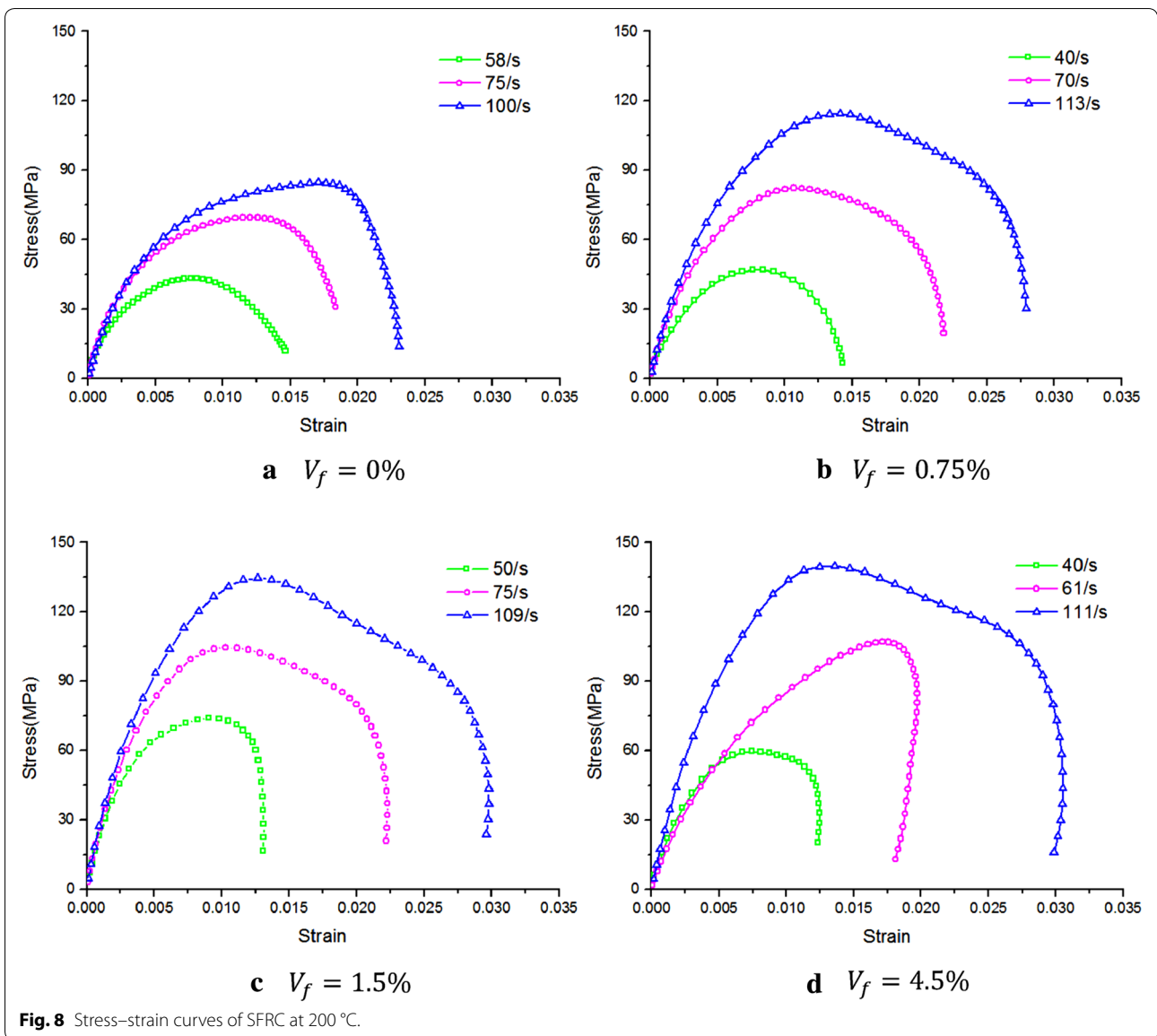


Fig. 8 Stress–strain curves of SFRC at 200 °C.

where $f(\dot{\epsilon}) = A + B\frac{\dot{\epsilon}}{\dot{\epsilon}_0}$ and $g(V_f) = 1 + C\left(\frac{V_f}{V_0}\right)^D$ are functions of strain rate $\dot{\epsilon}$ and fiber volume fraction V_f , respectively. A , B , C and D are material constants. $\dot{\epsilon}_0 = 1/s$ and $V_0 = 1\%$ are the reference strain rate and reference fiber volume fraction, respectively. As the strain rate effect of SFRC is related to temperature, it is assumed that the influence of temperature on the ultimate compressive strength is mainly reflected in parameters A and B :

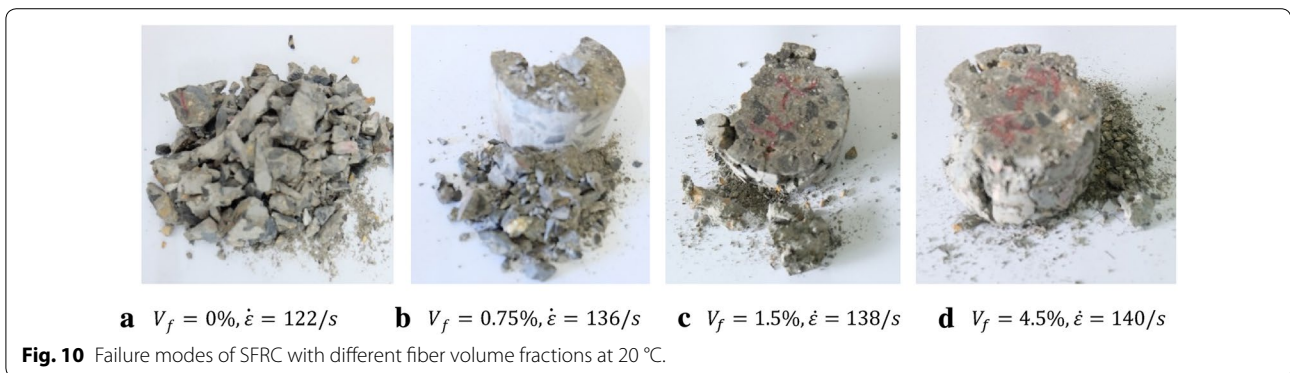
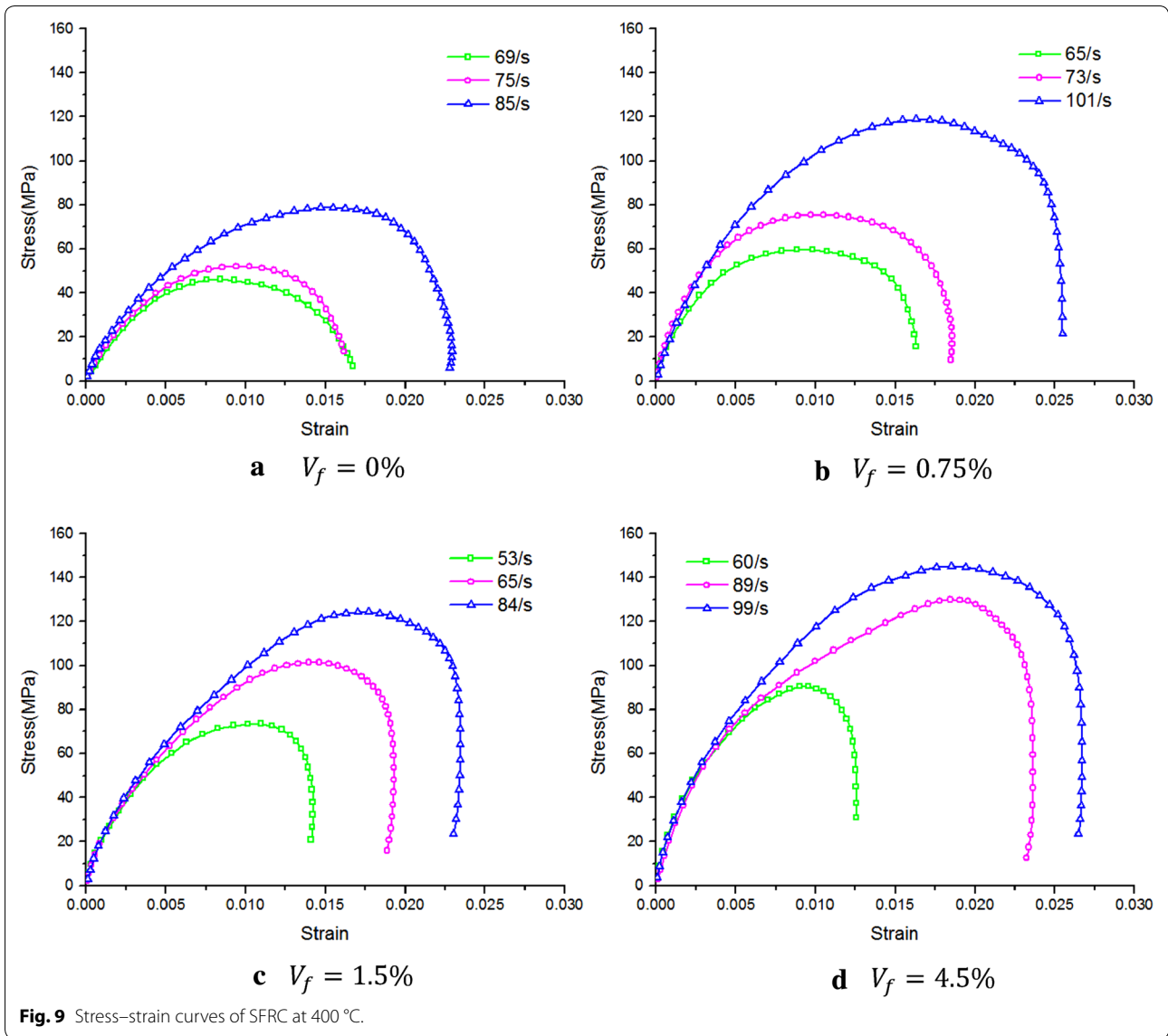
$$A = h_1(T), \tag{5}$$

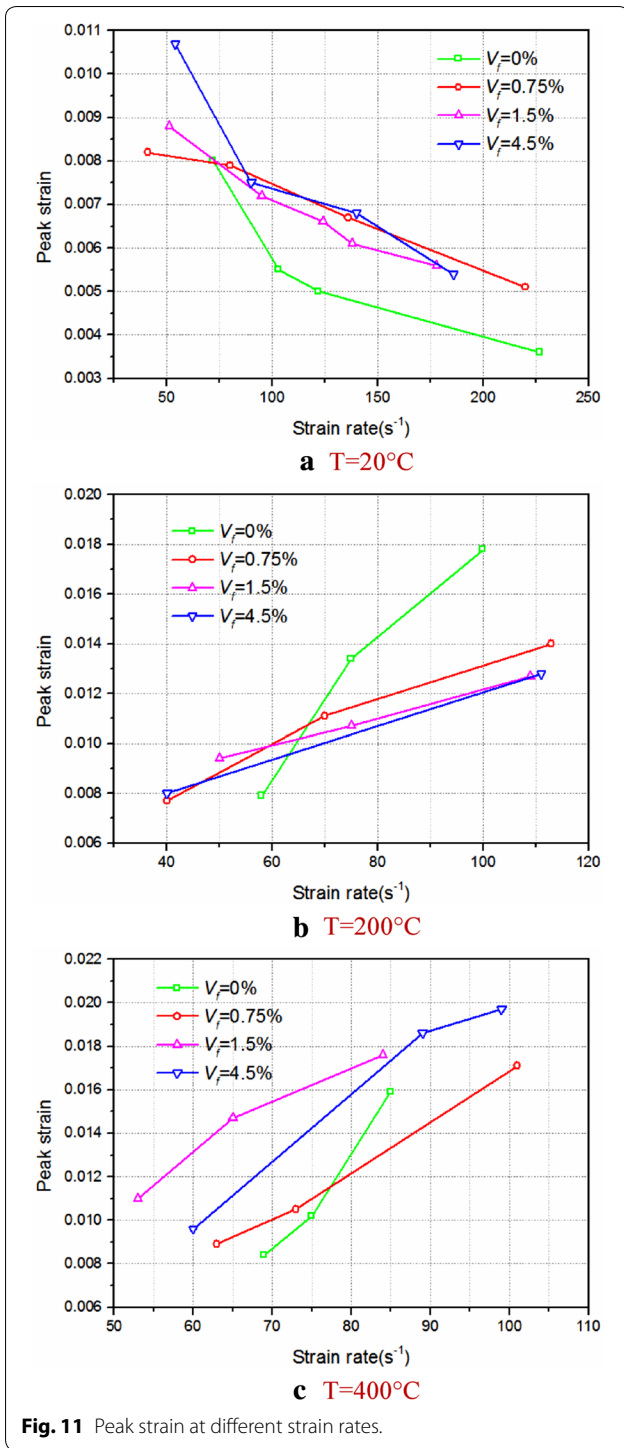
$$B = h_2(T). \tag{6}$$

4.2 Determination of Material Parameters

First, the influence of the strain rate on the ultimate compressive strength is discussed. Figure 15 shows the ultimate compressive strength–strain rate relationship at 20 °C for SFRC with fiber volume fraction of 0%. Then, $A = 45$ and $B = 0.193$ are determined for SFRC with fiber volume fraction of 0% at 20 °C.

Second, the influence of fiber volume fraction on the ultimate compressive strength of SFRC is discussed. Through the interpolation of experimental data, the ultimate compressive strengths of SFRC with different fiber volume fractions at 20 °C and strain rate of 138/s are obtained. Then, $C = 0.445$ and $D = 0.33$ are determined (Fig. 16).





As parameters A and B are functions of temperature, it is necessary to determine the values of parameters A and

B at different temperatures. Figure 17 shows the ultimate compressive strength–strain rate relationship of SFRC with different fiber volume fractions at different temperatures. Tables 2 and 3 present the values of parameters A and B of SFRC with different fiber volume fractions at different temperatures.

The values of parameters A and B at different temperatures have a significant linear relationship with temperature, as shown in Fig. 18. Therefore, the following formula can be adopted and the values of parameters a and b are presented in Table 4 and Fig. 19:

$$A = h_1(T) = 45 \times \left(1 + a \frac{T - T_0}{T_0} \right) \quad (7)$$

$$B = h_2(T) = 0.193 \times \left(1 + b \frac{T - T_0}{T_0} \right) \quad (8)$$

where a and b are material parameters and $T_0 = 20^\circ\text{C}$ is the reference temperature.

As the temperature effect is related to the fiber volume fraction, parameters A and B can be expressed as the relationship between the fiber volume fraction and the relevant material parameters presented in Table 5.

$$a = a' + b'c' \frac{V_f}{V_0} \quad (9)$$

$$b = a'' + b''c'' \frac{V_f}{V_0} \quad (10)$$

where a' , b' , c' , a'' , b'' , and c'' are material parameters.

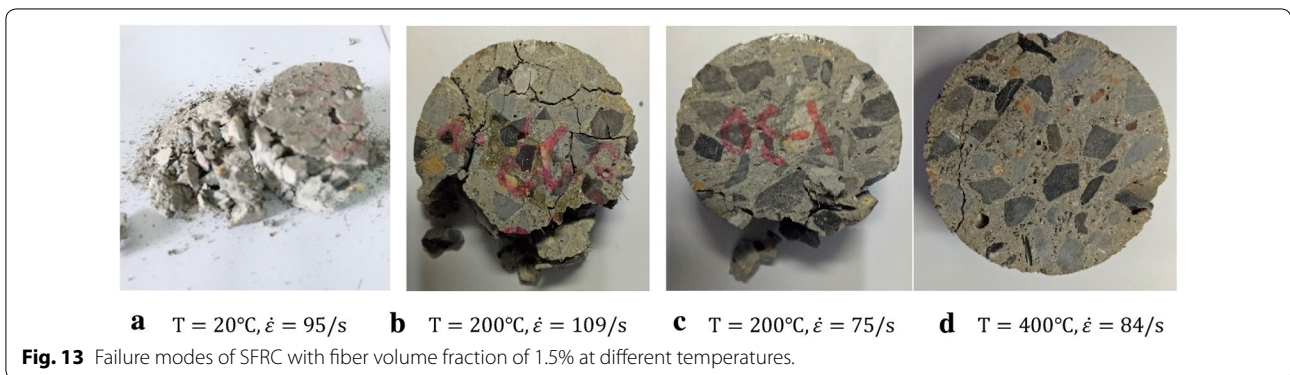
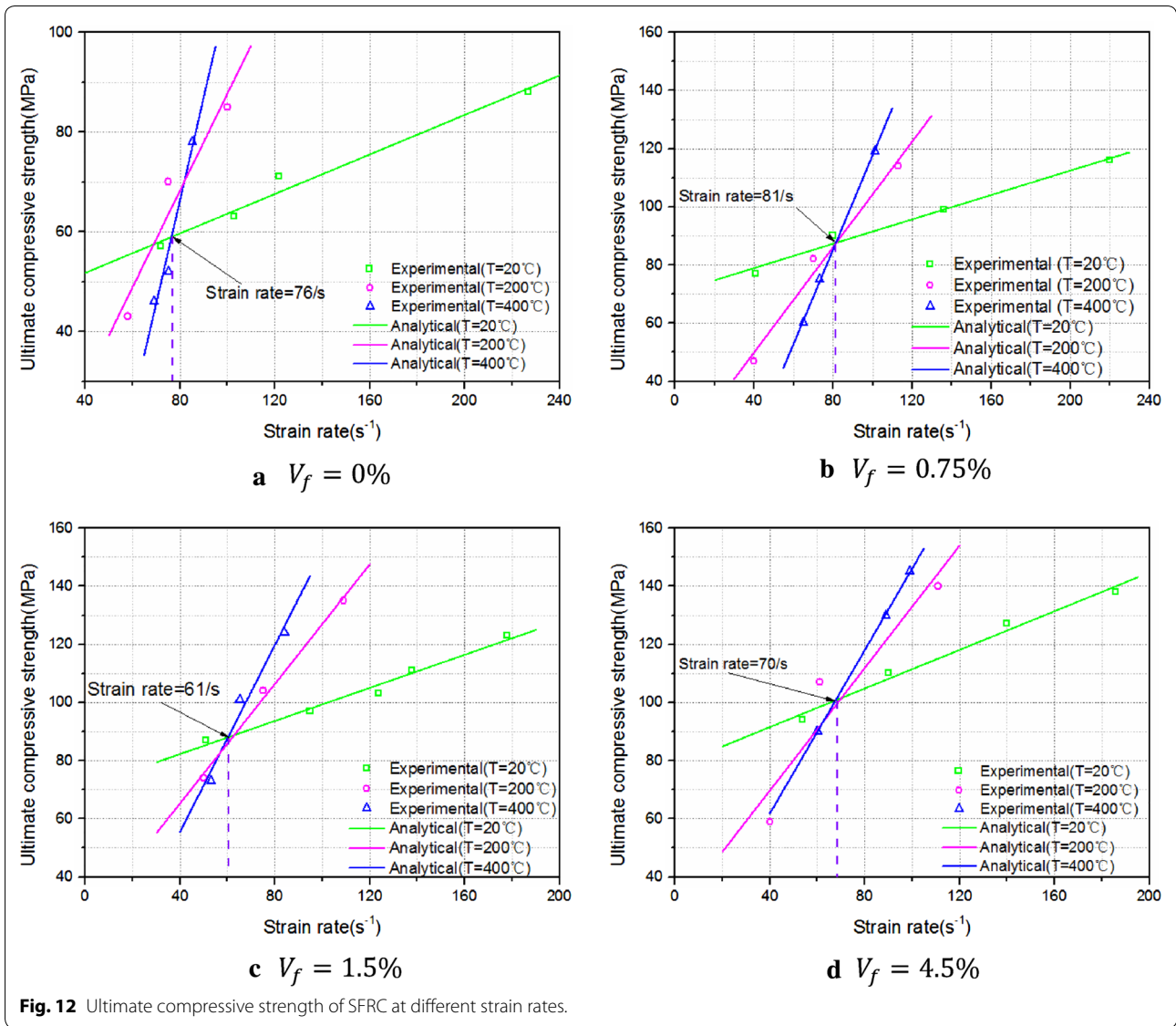
Then, the relationship between the ultimate compressive strength and strain rate, fiber volume fraction and temperature can be expressed as

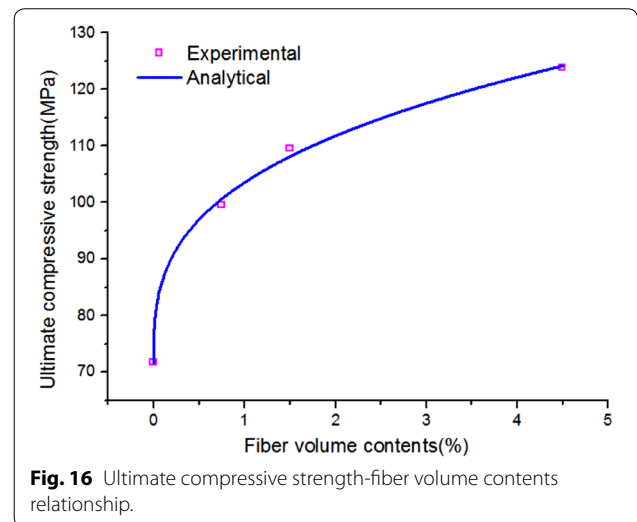
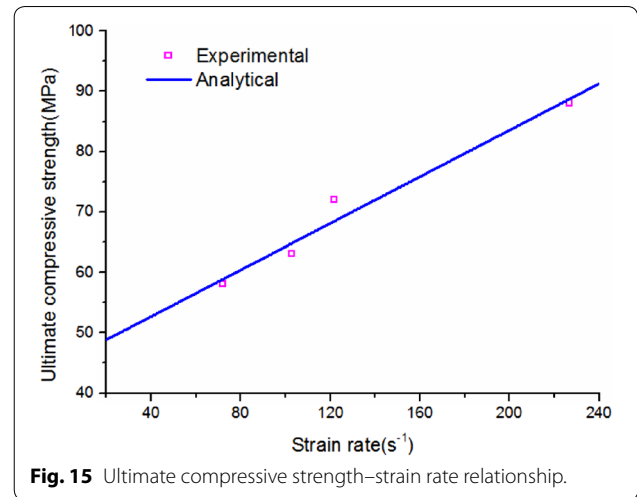
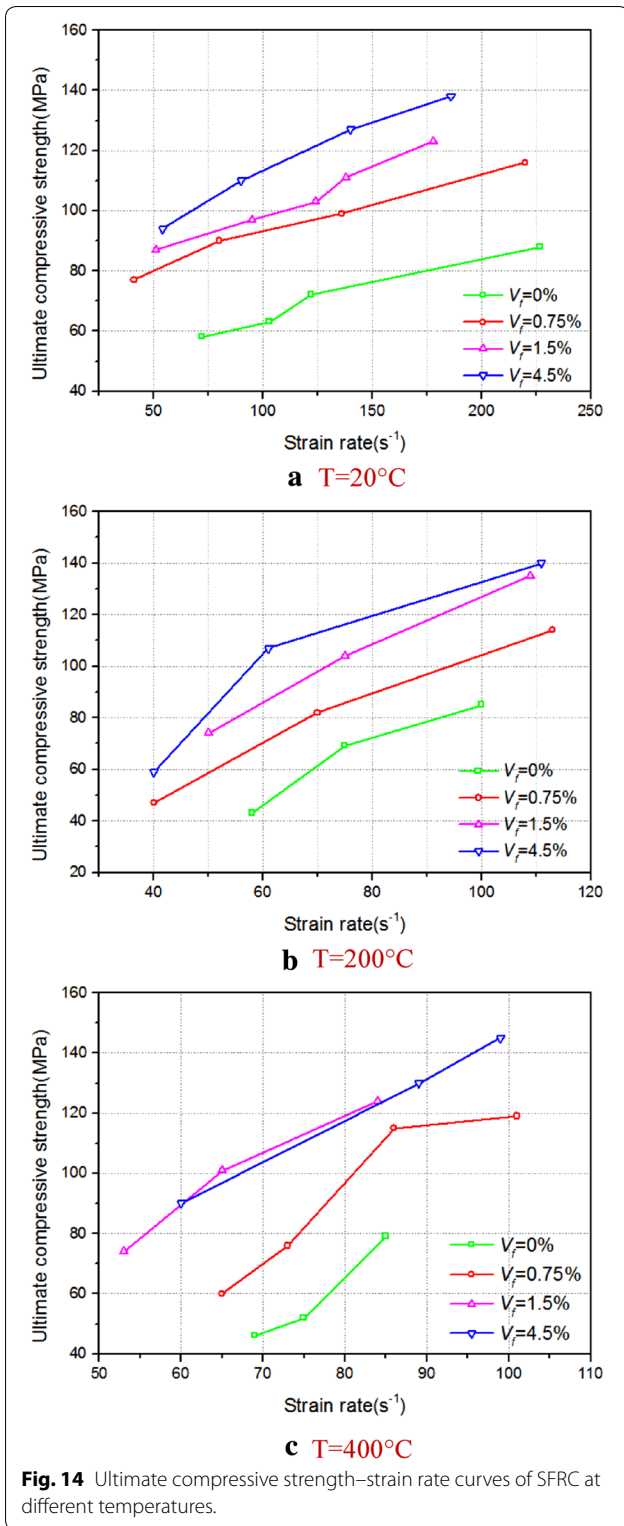
$$\begin{cases} \sigma_c = \left(A + B \frac{\dot{\epsilon}}{\dot{\epsilon}_0} \right) \left[1 + 0.445 \left(\frac{V_f}{V_0} \right)^{0.33} \right] \\ A = 45 \times \left[1 - \left(0.052 + 0.114 \times 0.225 \frac{V_f}{V_0} \right) \frac{T - T_0}{T_0} \right] \\ B = 0.193 \times \left[1 + \left(0.19 + 0.322 \times 0.213 \frac{V_f}{V_0} \right) \frac{T - T_0}{T_0} \right] \end{cases} \quad (11)$$

Figure 20 shows a comparison between the analytical and experimental data, and the results of the prediction are in good agreement with those of the experiment.

5 Conclusion

In this study, brass was used as a shaper to solve the problem of stress uniformity of SFRC specimens in SHPB experiments. The constant strain rate loading of an SFRC specimen under low strain rates can





be achieved by adjusting the size of the brass shaper, but the experimental results show that it is difficult to achieve a constant strain rate loading of SFRC specimen under high temperatures and high strain rates. The experimental data under constant strain rate loading show that the actual strain rate can be expressed as 1.35 times the average strain rate. Therefore, the strain rate corresponding to the experimental data under non-constant strain rate loading can be expressed by 1.35 times the average strain rate. This method is proposed to deal with the experimental data under non-constant strain rate loading conditions. SHPB experiments were conducted using SFRC with different fiber volume fractions

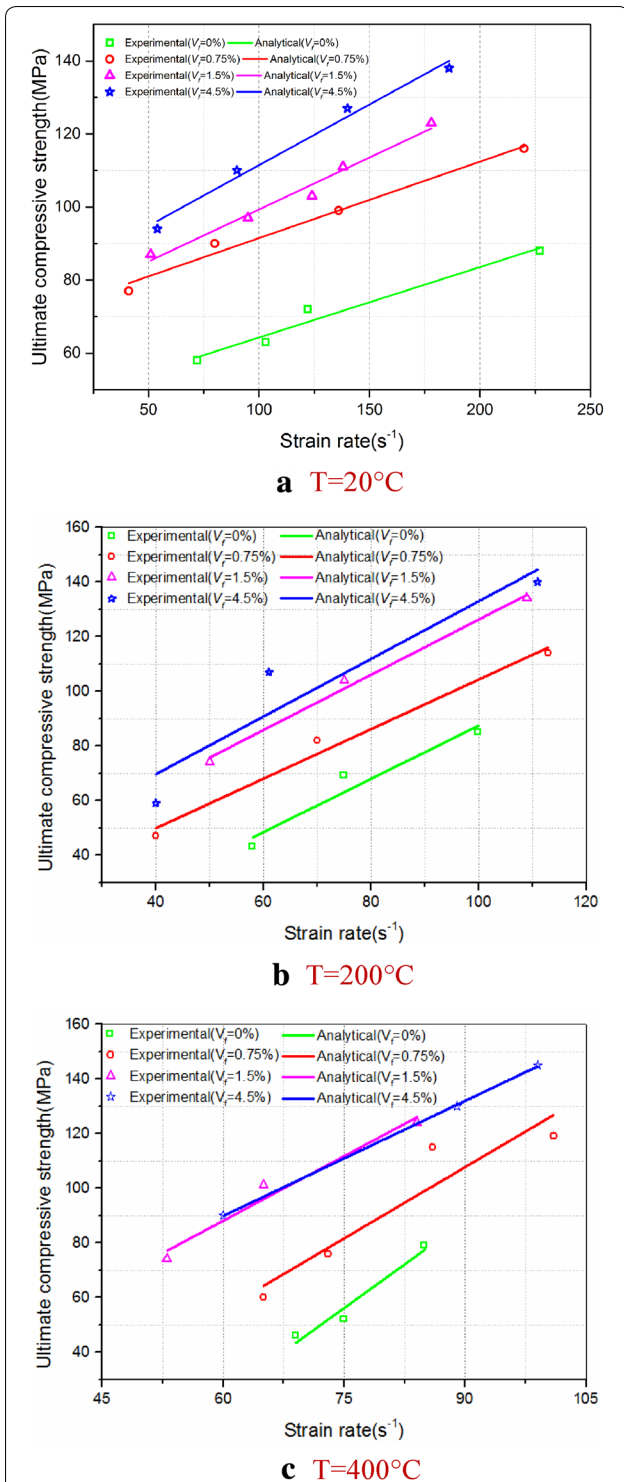


Fig. 17 Ultimate compressive strength–strain rate relationship of SFRC at different temperatures.

Table 2 Values of parameter A.

	$V_f = 0\%$	$V_f = 0.75\%$	$V_f = 1.5\%$	$V_f = 4.5\%$
20 °C	45	45	45	45
200 °C	-9.9	9.7	16.8	15.9
400 °C	-103.4	-34.7	-4.3	3.3

Table 3 Values of parameter B.

	$V_f = 0\%$	$V_f = 0.75\%$	$V_f = 1.5\%$	$V_f = 4.5\%$
20 °C	0.193	0.193	0.193	0.193
200 °C	0.973	0.645	0.67	0.61
400 °C	2.13	1.24	1.04	0.81

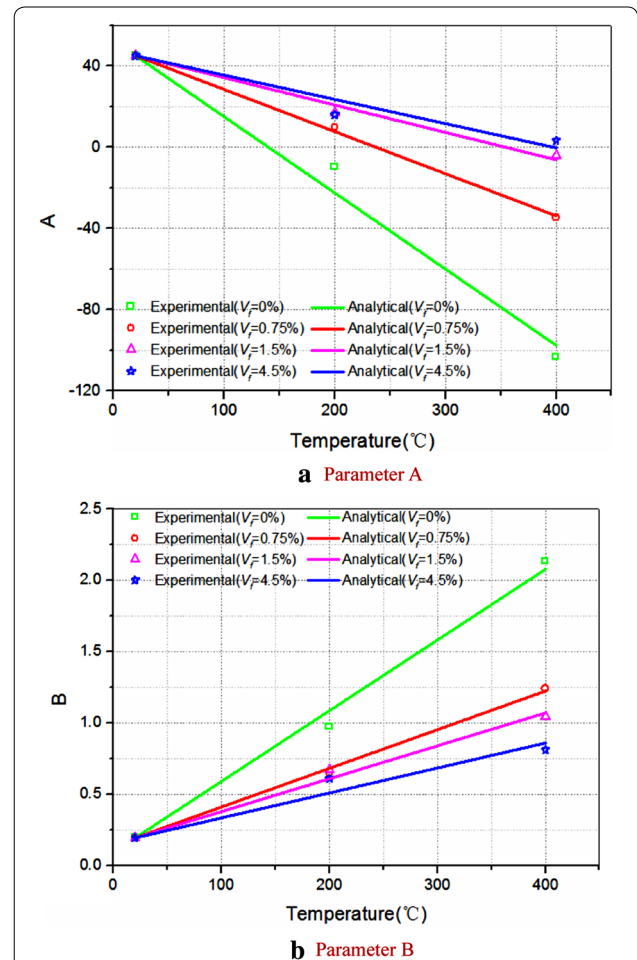


Fig. 18 Values of parameters A and B at different temperatures.

Table 4 Values of parameters a and b .

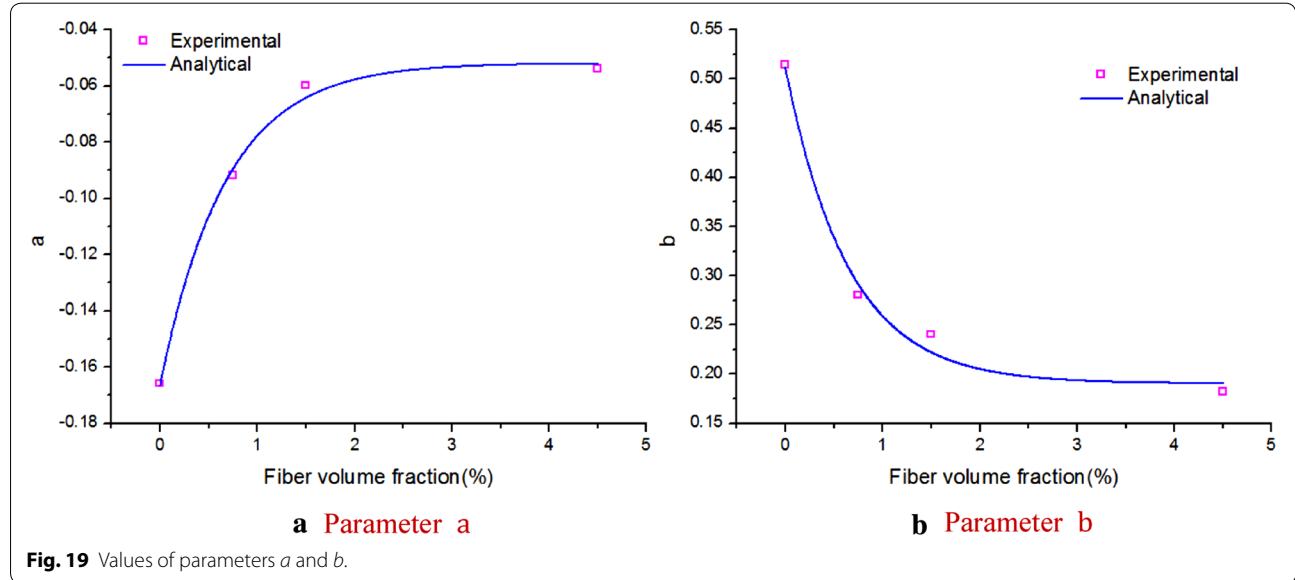
	$V_f = 0\%$	$V_f = 0.75\%$	$V_f = 1.5\%$	$V_f = 4.5\%$
a	-0.166	-0.092	-0.06	-0.054
b	0.514	0.28	0.24	0.182

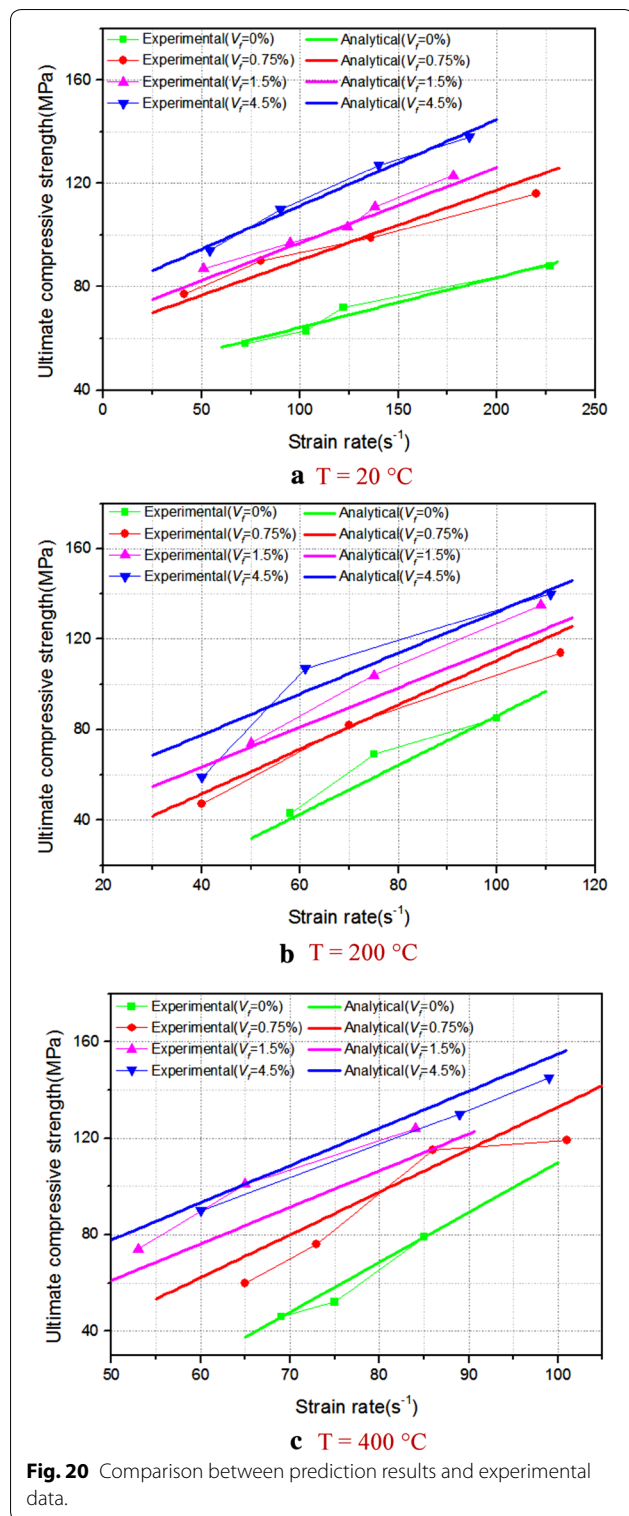
(0%, 0.75%, 1.5%, and 4.5%) at different temperatures (20 °C, 200 °C, and 400 °C) and different strain rates. The experimental results show that the addition of steel fiber significantly improves the toughness and strength of concrete. The peak strain decreases with the increase in strain rate at room temperature. However, the peak strain shows the opposite phenomenon at high temperature. Experimental results show that there is a strain rate threshold for SFRC. The strain rate thresholds for SFRC with fiber volume fractions of 0%, 0.75%, 1.5%, and 4.5% are 76/s, 81/s, 61/s, and 70/s, respectively. When the strain rate is less than the strain rate

Table 5 Values of SFRC material parameters.

a'	b'	c'	a''	b''	c''
-0.052	-0.114	0.225	0.19	0.322	0.213

threshold, the ultimate compressive strength decreases with the increase in temperature, indicating that it has a temperature softening effect. When the strain rate is greater than the strain rate threshold, the ultimate compressive strength increases with the increase in temperature, indicating that it has a temperature hardening effect. As the ultimate compressive strength is an important index to reflect the dynamic mechanical properties of SFRC, this study established the relationship between ultimate compressive strength and fiber volume fraction, strain rate, and temperature, and it is suitable for temperatures below 400 °C and strain rates lower than 250/s. The comparison between the





prediction results and experimental data confirms that they are in good agreement.

Acknowledgements

This work was supported by the National Natural Science Foundation of China (Grant Nos. 11802001, 11402266), the Foundation of Science and Technology on Transient Physics Laboratory (Grant No. 61426040403162604005) and the Open Foundation of Hypervelocity Impact Research Center of CARD (Grant No. 20181203).

Authors' contributions

Ruiyuan Huang: manuscript writing and test execution supervision. Shichao Li: test execution. Long Meng: supervisor of experiment and research. Dong Jiang and Ping Li: discussion to improve the quality of the research. All authors read and approved the final manuscript.

Funding

Not applicable.

Availability of data and materials

Not applicable.

Ethics approval and consent to participate

Not applicable.

Consent for publication

Not applicable.

Competing interests

The authors declare that they have no competing interests.

Author details

¹ Assistant Professor in Nanjing University of Science and Technology, Jiangsu 210094, China. ² Master Student in Nanjing University of Science and Technology, Jiangsu 210094, China. ³ Master Student in Nanjing University of Science and Technology, Jiangsu 210094, China. ⁴ Senior engineer in Beijing Institute of Space Long March Vehicle, Beijing 100076, China. ⁵ Assistant Professor in School of Management Science and Engineering, Anhui University of Technology, Maanshan 243032, Anhui, China.

Received: 7 March 2019 Accepted: 30 June 2020

Published online: 01 September 2020

References

Çavdar, A. (2012). A study on the effects of high temperature on mechanical properties of fiber reinforced cementitious composites. *Composites Part B (Engineering)*, 43(5), 2452–2463. <https://doi.org/10.1016/j.compositesb.2011.10.005>.

Chen, L., Fang, Q., Jiang, X., Ruan, Z., & Hong, J. (2015). Combined effects of high temperature and high strain rate on normal weight concrete. *International Journal of Impact Engineering*, 86, 40–56. <https://doi.org/10.1016/j.ijimpeng.2015.07.002>.

Dai, F., Huang, S., Xia, K., & Tan, Z. (2010). Some fundamental issues in dynamic compression and tension tests of rocks using split Hopkinson pressure bar. *Rock Mechanics and Rock Engineering*, 43(6), 657–666. <https://doi.org/10.1007/s00603-010-0091-8>.

Dilger, W. H., Koch, R., & Kowalczyk, R. (1984). Ductility of plain and confined concrete under different strain rates. *Aci Journal*, 81(1), 73–81.

Düğenci, O., Haktanir, T., & Altun, F. (2015). Experimental research for the effect of high temperature on the mechanical properties of steel

- fiber-reinforced concrete. *Construction and Building Materials*, 75, 82–88. <https://doi.org/10.1016/j.conbuildmat.2014.11.005>.
- El-Dieb, A. S. (2009). Mechanical, durability and microstructural characteristics of ultra-high-strength self-compacting concrete incorporating steel fibers. *Materials and Design*, 30(10), 4286–4292. <https://doi.org/10.1016/j.matdes.2009.04.024>.
- Frew, D. J., Forrestal, M. J., & Chen, W. (2002). Pulse shaping techniques for testing brittle materials with a split hopkinson pressure bar. *Experimental Mechanics*, 42(1), 93–106. <https://doi.org/10.1007/bf02411056>.
- Holschemacher, K., Mueller, T., & Ribakov, Y. (2010). Effect of steel fibres on mechanical properties of high-strength concrete. *Materials and Design*, 31(5), 2604–2615. <https://doi.org/10.1016/j.matdes.2009.11.025>.
- Kim, J., Lee, G. P., & Moon, D. Y. (2015). Evaluation of mechanical properties of steel-fibre-reinforced concrete exposed to high temperatures by double-punch test. *Construction and Building Materials*, 79, 182–191. <https://doi.org/10.1016/j.conbuildmat.2015.01.042>.
- Lau, A., & Anson, M. (2006). Effect of high temperatures on high performance steel fibre reinforced concrete. *Cement and Concrete Research*, 36(9), 1698–1707. <https://doi.org/10.1016/j.cemconres.2006.03.024>.
- Li, W., Luo, Z., Wu, C., Tam, V. W. Y., Duan, W. H., & Shah, S. P. (2017a). Experimental and numerical studies on impact behaviors of recycled aggregate concrete-filled steel tube after exposure to elevated temperature. *Materials and Design*, 136, 103–118. <https://doi.org/10.1016/j.matdes.2017.09.057>.
- Li, J., Wu, C., Hao, H., & Su, Y. (2017b). Experimental and numerical study on steel wire mesh reinforced concrete slab under contact explosion. *Materials and Design*, 116, 77–91. <https://doi.org/10.1016/j.matdes.2016.11.098>.
- Li, W. M., Xu, J. Y., Shen, L. J., & Li, Q. (2008). Study on 100 mm-diameter SHPB techniques of dynamic stress equilibrium and nearly constant strain rate loading. *Journal of Vibration and Shock*, 27(2), 129–132. <https://doi.org/10.3969/j.issn.1000-3835.2008.02.030>.
- Liu, S., & Xu, J. (2013). Study on dynamic characteristics of marble under impact loading and high temperature. *International Journal of Rock Mechanics and Mining Sciences*, 62, 51–58. <https://doi.org/10.1016/j.ijrmms.2013.03.014>.
- Lv, T. H., Chen, X. W., & Chen, G. (2018). The 3D meso-scale model and numerical tests of split Hopkinson pressure bar of concrete specimen. *Construction and Building Materials*, 160, 744–764. <https://doi.org/10.1016/j.conbuildmat.2017.11.094>.
- Pan, Z., Sanjayam, J. G., & Collins, F. (2014). Effect of transient creep on compressive strength of geopolymer concrete for elevated temperature exposure. *Cement and Concrete Research*, 56(2), 182–189. <https://doi.org/10.1016/j.cemconres.2013.11.014>.
- Poon, C. S., Shui, Z. H., & Lam, L. (2004). Compressive behavior of fiber reinforced high-performance concrete subjected to elevated temperatures. *Cement and Concrete Research*, 34(12), 2215–2222. <https://doi.org/10.1016/j.cemconres.2004.02.011>.
- Ravichandran, G., & Subhash, G. (1994). Critical appraisal of limiting strain rates for compression testing of ceramics in a split Hopkinson pressure bar. *Journal of the American Ceramic Society*, 77(1), 263–267. <https://doi.org/10.1111/j.1151-2916.1994.tb06987.x>.
- Siddique, R., & Kaur, D. (2012). Properties of concrete containing ground granulated blast furnace slag (GGBFS) at elevated temperatures. *Journal of Advanced Research*, 3(1), 45–51. <https://doi.org/10.1016/j.jare.2011.03.004>.
- Song, P. S., & Hwang, S. (2004). Mechanical properties of high-strength steel fiber-reinforced concrete. *Construction and Building Materials*, 18(9), 669–673. <https://doi.org/10.1016/j.conbuildmat.2004.04.027>.
- Song, Z., & Lu, Y. (2012). Mesoscopic analysis of concrete under excessively high strain rate compression and implications on interpretation of test data. *International Journal of Impact Engineering*, 46, 41–55. <https://doi.org/10.1016/j.ijimpeng.2012.01.010>.
- Su, H., Xu, J., & Ren, W. (2014). Experimental study on the dynamic compressive mechanical properties of concrete at elevated temperature. *Material and Design*, 2014(56), 579–588. <https://doi.org/10.1016/j.matdes.2013.11.024>.
- Tai, Y. S., Pan, H. H., & Kung, Y. N. (2011). Mechanical properties of steel fiber reinforced reactive powder concrete following exposure to high temperature reaching 800 °C. *Nuclear Engineering and Design*, 241(7), 2416–2424. <https://doi.org/10.1016/j.nucengdes.2011.04.008>.
- Tao, J. L., Chen, Y. Z., Tian, C. J., Chen, G., Li, S. Z., Huang, X. C., et al. (2005). Investigation of the effect of strain rate history on the stress-strain curves. *Explosion and Shock Waves*, 25(1), 80–84. <https://doi.org/10.3321/j.issn:1001-1455.2005.01.015>.
- Wang, Z., & Hao, S. (2017). Study on dynamic compressive mechanical properties and failure modes of heat-treated granite. *Latin American Journal of Solids and Structures*, 14(4), 657–673. <https://doi.org/10.1590/1679-78253342>.
- Wang, Y. T., Liu, D. S., Li, S. L., & Jiang, Y. Q. (2014). Dynamic performance of concrete based on a $\Phi 75$ mm SHPB system under high temperature. *Journal of Vibration & Shock*, 33(17), 12–17. <https://doi.org/10.13465/j.cnki.jvs.2014.17.003>.
- Wang, Z. L., Liu, Y. S., & Shen, R. F. (2008). Stress-strain relationship of steel fiber-reinforced concrete under dynamic compression. *Construction and Building Materials*, 22(5), 811–819. <https://doi.org/10.1016/j.conbuildmat.2007.01.005>.
- Wang, S., Zhang, M. H., & Quek, S. T. (2012). Mechanical behavior of fiber-reinforced high-strength concrete subjected to high strain-rate compressive loading. *Construction and Building Materials*, 31, 1–11. <https://doi.org/10.1016/j.conbuildmat.2011.12.083>.
- Wu, W., Zhang, W., & Ma, G. (2010). Mechanical properties of copper slag reinforced concrete under dynamic compression. *Construction and Building Materials*, 24(6), 910–917. <https://doi.org/10.1016/j.conbuildmat.2009.12.001>.
- Xiao, J., Li, L., Shen, L., & Poon, C. S. (2015). Compressive behaviour of recycled aggregate concrete under impact loading. *Cement and Concrete Research*, 71, 46–55. <https://doi.org/10.1016/j.cemconres.2015.01.014>.
- Xu, Y., Wong, Y. L., Poon, C. S., & Anson, M. (2001). Impact of high temperature on PFA concrete. *Cement and Concrete Research*, 31(7), 1065–1073. [https://doi.org/10.1016/S0008-8846\(01\)00513-0](https://doi.org/10.1016/S0008-8846(01)00513-0).
- Yang, J. M., Yoo, D. Y., Kim, Y. C., & Yoon, Y. S. (2017). Mechanical properties of steam cured high-strength steel fiber-reinforced concrete with high-volume blast furnace slag. *International Journal of Concrete Structures and Materials*, 11(2), 391–401. <https://doi.org/10.1007/s40069-017-0200-0>.
- Zhu, J., Hu, S., & Wang, L. (2009). An analysis of stress uniformity for concrete-like specimens during shpb tests. *International Journal of Impact Engineering*, 36(1), 61–72. <https://doi.org/10.1016/j.ijimpeng.2008.04.007>.

Publisher's Note

Springer Nature remains neutral with regard to jurisdictional claims in published maps and institutional affiliations.